Nanomed Res J 10(3):295-305, Summer 2025

RESEARCH ARTICLE

Tyrosinase inhibition and angiogenesis studies of zinc oxide nanoparticles green synthesized using aqueous extract of *Peucedanum knappii*

Parisa Sarkhail[1*], Sorour Foroughian[2], Mahdi Gholami[3], Latifeh Navidpour[4]

[1] Medicinal Plants Research Center, The Institute of Pharmaceutical Sciences, Faculty of Pharmacy, Tehran University of Medical Sciences, Tehran, Iran

[2] Department of Pharmacognosy, Faculty of Pharmacy, Tehran University of Medical Sciences, Tehran, Iran

[3] Department of Toxicology & Pharmacology, Faculty of Pharmacy, Toxicology and Poisoning Research Center, Tehran University of Medical Sciences, Tehran, Iran

[4] Department of Medicinal Chemistry, Faculty of Pharmacy, Tehran University of Medical Sciences, Tehran, Iran

ARTICLE INFO

Article History:
Received 18 Jun 2025
Accepted 23 Aug 2025
Published 01 Sep 2025

Keywords:
Angiogenesis
CAM assay
Peucedanum knappii
Tyrosinase inhibition
ZnO nanoparticles

ABSTRACT

To investigate the anti-tyrosinase and angiogenic properties of zinc oxide nanoparticles (ZONPs), an aqueous extract prepared from the aerial parts of Peucedanum knappii Bornm., known to be rich in glycosylated phenolics and polyphenolics, was employed for the green synthesis of ZONPs. The ZONPs were produced by adding a Zn salt solution to the aqueous of the plant. High–performance liquid chromatography (HPLC) was employed to examine chromatographic changes in the extract before and after nanoparticle formation. The synthesized ZONPs were comprehensively characterized using UV–Visible spectroscopy, Fourier transform infrared (FTIR) spectroscopy, scanning electron microscopy (SEM), and X–ray diffraction (XRD). The effect of ZONPs on tyrosinase enzyme activity was assessed through an in vitro mushroom tyrosinase inhibition assay, whereas their angiogenic potential was evaluated in vivo using the chicken chorioallantoic membrane (CAM) assay. The results confirmed the successful green synthesis of ZONPs utilizing P. knappii aqueous extract (PAE). HPLC analysis indicated that multiple phytochemicals present in PAE contributed to nanoparticle formation. Characterization data revealed that the ZONPs exhibited a hexagonal crystalline ZnO structure with an average crystallite size of 19.98 nm. The nanoparticles showed notable anti-tyrosinase activity, with an IC_{50} value of 143.28 µg/ml, and promoted angiogenesis in the CAM assay at concentrations between 125 and 250 µg/ml without inducing toxicity. Overall, these findings demonstrate that PAE acts as an effective reducing, capping, and stabilizing agent in the green synthesis of ZONPs, which possess promising biological properties for potential applications in skin-whitening cosmetics and wound-healing formulations.

How to cite this article
Sarkhail P., Foroughian S., Gholami M., Navidpour L. Tyrosinase inhibition and angiogenesis studies of zinc oxide nanoparticles green synthesized using aqueous extract of Peucedanum knappii . Nanomed Res J, 2025; 10(3): 295-305. DOI: 10.22034/nmrj.2025.03.008

INTRODUCTION

In recent decades, nanotechnology has created a new path in the design and synthesis of materials in various fields, including chemistry, medicine, agriculture, electronics, and physics. Compared with bulk materials, nanoparticles (NPs) display distinct physicochemical and biological characteristics that significantly enhance their performance in various scientific and technological domains [1, 2]. Among them, metal oxide nanoparticles have gained considerable attention for their crucial roles in biomedical applications, particularly in drug delivery, biosensors and imaging technology [3, 4]. Despite their potential, conventional chemical synthesis methods for

* Corresponding Author Email: *sarkhail@sina.tums.ac.ir*

nanoparticles often rely on hazardous chemicals and conditions, leading to environmental and biological risk. To overcome these limitations, researchers have increasingly focused on green synthesis strategies, which are recognized for their economic feasibility, non-toxicity, simplicity, and environmental sustainability [5–7].

Recent studies indicate that nanoparticles (NPs) synthesized using plants exhibit faster formation and greater stability compared to those produced by other organisms. The shape and size of NPs produced by plants differ from those created by various organisms. The synthesis of nanoparticles using plant-based systems provides multiple benefits compared to other biological sources such as bacteria, algae, fungi, and yeasts, as it tends to be safer, more environmentally friendly, economical, and sustainable [7, 8].

In green synthesis, the active biomolecules found in plant extracts serve as both reducing and stabilizing agents for metal nanoparticles, allowing their formation without generating harmful by-products. For example, when aqueous plant extracts rich in free hydroxyl (OH) groups from phenolic and polyphenolic compounds are added to zinc salts such as acetates, nitrates, or sulfates, zinc–phenolic complexes are produced. These complexes promote the reduction of Zn^{2+} ions and facilitate the synthesis of zinc-based nanoparticles [8–10]. Zinc oxide is acknowledged as a safe substance by the U.S. Food and Drug Administration (FDA), and zinc oxide nanoparticles (ZONPs) are classified by the FDA as a "GRAS" (Generally Recognized As Safe) ingredient [10]. Among metal oxide NPs, ZONPs are generally utilized in many biomedical fields because of their unique physicochemical characteristics, low toxicity, and good biocompatibility [11]. Numerous reports indicate that ZONPs derived from polyphenolic extracts exhibit significant antimicrobial, anticancer, antioxidant, anti-aging, anti-diabetic, anti-inflammatory, and angiogenic effects [12–15].

The process of wound healing involves four partially overlapping phases: hemostasis, inflammation, proliferation, and remodeling. Throughout these phases, the body repairs damaged cells and tissues. In the proliferative phase, angiogenesis increases oxygen and nutrient flow to the wound, accelerating healing. Moreover, post-inflammatory hyperpigmentation frequently occurs in patients with wounds, particularly in cases of burn injuries, causing dark spots or patches on the skin due to excessive melanin production during the healing process [16, 17].

Over the past decade, several studies have individually demonstrated that ZONPs can enhance wound healing and inhibit tyrosinase activity at low doses [15, 18]. Currently, there is a lack of research evaluating the effects of ZONPs synthesized through green method on both tyrosinase activity and angiogenesis. In this research, ZONPs were synthesized via a green method using an aqueous extract from the aerial parts of *Peucedanum knappii*, a native fennel species rich in glycosylated phenolics and polyphenolics [19]. The synthesized nanoparticles were characterized through spectroscopic and microscopic analyses, including UV–Vis, FTIR, SEM, and XRD. Their biological activity was assessed by examining their inhibitory effects on tyrosinase *in vitro* and their influence on angiogenesis *in vivo*, to evaluate their potential for treating hyperpigmentation and enhancing wound healing.

MATERIALS AND METHODS

Chemicals

Mushroom tyrosinase, kojic acid, potassium dihydrogen phosphate, dipotassium hydrogen phosphate, dimethyl sulfoxide (DMSO), zinc acetate dihydrate ($Zn(CH_3COO)_2{\cdot}2H_2O$), and sodium hydroxide (NaOH) were obtained from Sigma-Aldrich (USA). All other analytical-grade reagents and solvents were purchased from Merck (Germany).

Preparation of Aqueous Plant Extract

Aerial parts of *Peucedanum knappii* Bornm. were collected from their natural habitat in West Azerbaijan Province, Iran, and authenticated at the Herbarium of the Department of Pharmacognosy, Tehran University of Medical Sciences (TUMS), where a voucher specimen (No. 6669 TEH) was deposited. The dried plant material was finely powdered, and 30 g of the powder was subjected to percolation using a methanol–water mixture (80:20, v/v). The obtained hydroalcoholic extract was concentrated under reduced pressure using a rotary evaporator. The resulting residue was dissolved in distilled water and sequentially partitioned with hexane, dichloromethane, ethyl acetate, and finally water. The aqueous fraction was filtered through Whatman No. 1 filter paper, freeze-dried, and stored at low temperature until further use.

Green Synthesis of ZONPs.

Based on the established green synthesis protocol for metal oxide nanoparticles (12), ZONPs were produced using zinc acetate as a precursor and *P. knappii* aqueous extract (PAE) as the reducing and stabilizing agent. A 0.1 M zinc acetate solution was prepared with double-distilled water, and 190 ml of this solution was heated to 80 °C under constant stirring. To this, 10 mL of 0.1 M PAE was gradually introduced, followed by 12 ml of 4 M NaOH to attain a reaction pH of 12.5. After incubation at room temperature for 24 hours, a white precipitate was formed. The product was centrifuged at 5000 rpm for 20 minutes (repeated three times) and washed thoroughly with distilled water and ethanol to remove residual impurities. The purified material was air-dried for 24 hours and then oven-dried at 100 °C for 4 hours, yielding 0.67 g of white ZONP powder.

HPLC Analysis

Upon completion of nanoparticle synthesis, the supernatant containing the residual *P. knappii* aqueous extract (RPAE) was collected. Both PAE and RPAE were analyzed using a Knauer 1260 series HPLC sysem equipped with a diode array detector (DAD) and C18 column (4.6 mm × 250 mm, 5 µm). Stock solutions of PAE and RPAE were prepared by dissolving 1 mg of each dried extract in 1 mL of deionized water. The HPLC mobile phase consisted of solvent A (water) and solvent B (methanol), delivered at a flow rate of 1 ml/min. A linear gradient program was applied as follows: 0–10 min, 100% A; 10–20 min, 80% A and 20% B; and 20–60 min, 100% B. Detection was performed using a multi-wavelength detector set at 254 nm, with the column maintained at 25 °C. Before injection, all samples were filtered through 0.45 µm syringe filters. The injection volume for each sample was 20 µl.

UV–Visible Spectroscopy Analysis

The formation of ZONPs was confirmed by recording their UV–Vis absorption spectra using a Shimadzu UV–Vis Spectrophotometer-1800 (Japan). The nanoparticles were dispersed in deionized water and subjected to ultrasonic irradiation for 15 minutes to ensure uniform suspension. Absorption spectra of both PAE and the synthesized nanoparticles were measured over a wavelength range of 200–800 nm at room temperature.

FT-IR Spectroscopy Analysis

FT–IR analysis was conducted using a Bruker FT–IR spectrometer to identify the functional groups present in ZONPs and the phytochemicals involved in their reduction and stabilization. The spectra of both PAE and the synthesized ZONPs were recorded using the KBr pellet method over a wavenumber range of 4000–400 cm^{-1}. This analysis allows the detection of characteristic absorption bands corresponding to specific functional groups that play a role in nanoparticle formation and stabilization.

Scanning Electron Microscopy (SEM) Analysis

SEM analysis was performed on a HITACHI S–4500 to study the size and morphology of ZONPs. The nanoparticles were first suspended in 96% ethanol and sonicated for 15 minutes to ensure uniform dispersion. A small portion of the suspension was then deposited onto a surface, and the solvent was allowed to evaporate at room temperature before capturing SEM images.

X-Ray Diffraction (XRD) Analysis

The crystalline structure, size, and purity of ZONPs were analyzed by X–ray diffraction (XRD) using a PHILIPS X'Pert Pro (PW3064) diffractometer. XRD patterns were obtained at room temperature with Cu Kα radiation (λ = 1.54184 Å), under a voltage of 30 kV and a current of 30 mA, scanning the 2θ angular range of 20–100°.

Biological Assays

Tyrosinase Inhibitory Activity Assay

To assess the capacity of ZONPs to inhibit the tyrosinase activity, a spectrophotometric method was employed in 96-well plates [19]. A total of 200 µl assay mixture was prepared, containing ZONPs at concentrations of 62.5–500 µg/ml, 50 mM phosphate buffer (pH 6.8), and 125 U/ml mushroom tyrosinase. The mixture was pre-incubated at 37 °C for 10 minutes, after which 2 mM L-tyrosine was added to start the reaction. The reaction proceeded at room temperature for 30 minutes, and the absorbance was measured at 475 nm. Kojic acid was included as a standard tyrosinase inhibitor for comparison, and all assays were performed in triplicate.

In vivo Chicken Chorioallantoic Membrane (CAM) Assay

The chick chorioallantoic membrane (CAM)

model is widely used to investigate angiogenesis in both wound healing and tumor biology [20, 21]. Twenty fertilized Hy-Line W–80 eggs were first disinfected with alcohol and randomly assigned to five groups: a vehicle control group (PBS), a negative control group (1% DMSO), and three treatment groups receiving ZONPs at 125, 250, or 500 µg/ml. The eggs were incubated at 37.5 °C with 60-65% humidity and automatically rotated. On day 3 of incubation, under sterile conditions, a small hole was made at the bottom of each egg, and 3 ml of albumen was removed using a syringe; the hole was then sealed with adhesive tape. A 1 cm^2 window was created on the side of each egg, which was subsequently sealed and returned to the incubator maintained at 37.5 °C and 70% humidity. On day 7, 10 µl of the assigned sample was applied to each experimental group under aseptic conditions. The windows were resealed, and the eggs were incubated for an additional 48 hours. On day 9, eggshells were carefully removed, and all CAMs were examined both macroscopically and microscopically. Quantitative measurements of blood vessel number and length were performed using ImageJ software, based on images captured with an Optica SZM-LED1 research stereomicroscope (Italy). Embryo viability was reassessed on day 11 to finalize the study.

Statistical Analysis

Statistical evaluation of the CAM assay (n = 4) was carried out using one-way ANOVA, followed by Dunnett's post hoc test. For the tyrosinase inhibition assay (n = 3), linear regression analysis was employed. Data are expressed as mean ± standard deviation, and differences were considered statistically significant at $p < 0.05$. All analyses were performed using GraphPad Prism 8 software. Additionally, the particle size distribution of ZONPs was plotted using Microsoft Excel.

RESULTS

HPLC Analysis Chromatogram of PAE Before and After Green Synthesis

In this study, HPLC was used to observe the changes in PAE chromatogram before and after ZONPs formation. The HPLC chromatograms of PAE (Figure S1a) showed three major peaks at 19.5, 29.5, and 42 min, along with other peaks between 16 and 47 min, while the chromatogram of RPAE (Figure S1b) did not show these peaks. The absence of these peaks in the RPAE chromatogram indicates the involvement of these biomolecules in the synthesis of ZONPs. However, the analysis and structural elucidation of these compounds were not performed in this study.

Visual Observation Green Synthesis of ZONPs

UV–Visible Absorption Spectral Analysis of PAE and the Synthesized ZONPs

The pale white ZONPs were produced from PAE using a green synthesis approach. While the precise mechanism behind nanoparticle formation remains unclear, it is understood that during the green synthesis of ZONPs, zinc ions (Zn^{2+}) interact with components of the extract, promoting their reduction to ZnO. To confirm the visual observations of ZONPs formation, UV–Vis absorption spectrophotometric measurements were carried out on the aqueous extract and the suspension of ZONPs in deionized water. The UV–Vis analysis of the aqueous extract showed absorption peaks at 254 and 320 nm, suggesting the presence of aromatic compounds, including phenolics and flavonoids [22], as shown in Figure 1a. A maximum absorption peak was observed at 373 nm for ZONPs, as shown in Figure 1b.

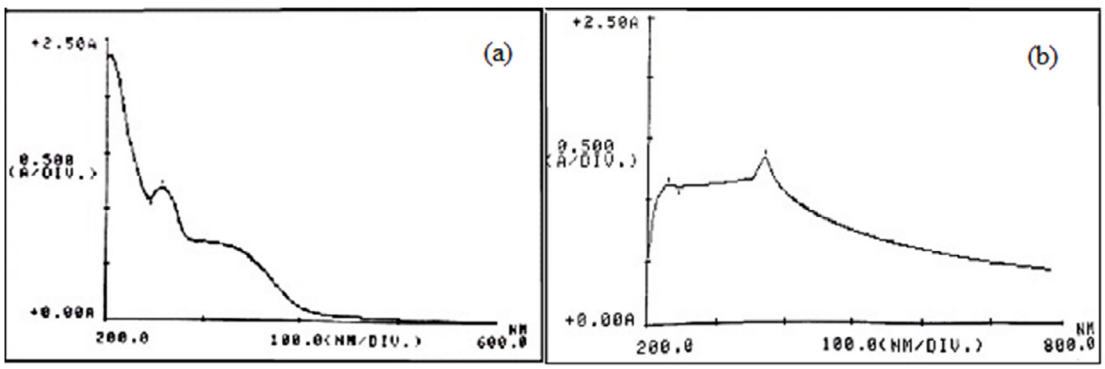

Fig. 1. UV–Vis absorption spectra of (a) *P. knappii* aqueous extract (PAE) and (b) the green synthesized ZONPs.

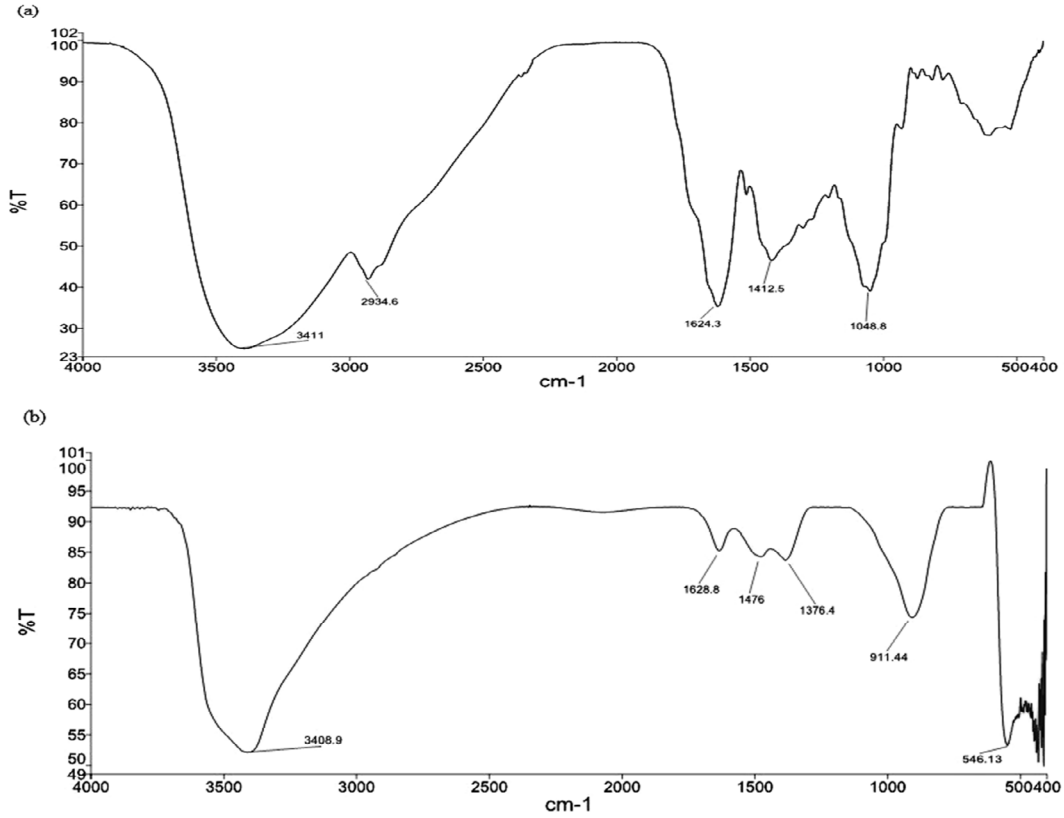

Fig. 2. FT-IR spectra recoded from KBr pellets containing dry powder samples of (a) *P. knappii* aqueous extract (PAE) and (b) the green synthesized ZONPs.

FT-IR Analysis of PAE and the Synthesized ZONPs

FT-IR studies were conducted on PAE and synthesized ZONPs to identify potential biomolecules in PAE and the functional groups responsible for the reduction and stabilization of NPs (Figure 2).

The broad absorption bands at 3408 and 3411 cm^{-1} are attributed to O–H stretching, indicating the presence of hydroxyl groups in phenolic, polyphenolic, and glycoside compounds. The band observed at 2934 cm^{-1} corresponds to C–H stretching vibrations. Peaks around 1700 cm^{-1} are characteristic of C=O stretching. The bands at 1624 cm^{-1} and 1628 cm^{-1} are associated with C=C stretching vibrations within the aromatic ring system, while the sharp, intense peak at 1412 cm^{-1} further confirms aromatic C=C stretching. Finally, the absorption near 1048 cm^{-1} can be assigned to C–O stretching or C–H bending in alkane groups (Figure 2a). The FT-IR spectrum of ZONPs revealed that the OH stretching plays a major role during the formation of ZONPs (Figure 2b). The frequencies of bands between 1300–1700 cm^{-1} clearly decrease in intensity in the ZONPs spectrum due to the attachment of the functional groups such as C=O, C=C, and C–O. The band at 911 cm^{-1} may indicate the presence of –CH stretching vibrations that are linked to ZnO. In addition, the absorption bands between 400 and 500 cm^{-1} are assigned to the successful Zn–O formation in the ZONPs.

SEM Analysis

SEM was employed to examine the morphology and particle size of the green synthesized ZONPs. According to the SEM images (Figure 3a), the surface morphology and shape of ZONPs were almost spherical and clearly showed particle aggregation, which probably occurred during the drying process. The nanoparticle sizes were found between 20 and 80 nm, as calculated using ImageJ software. The particle size distribution histograms indicate that the green-synthesized ZONPs have an average size of approximately 44 nm (Figure 3b).

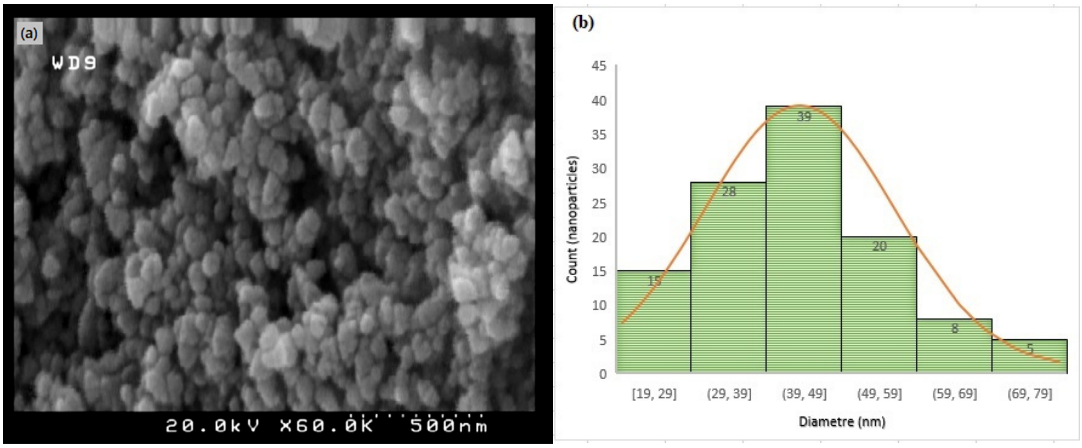

Fig. 3. (a) SEM images of the green synthesized ZONPs. (b)The particle size distribution graph of ZONPs with the average diametre ≈ 44 nm.

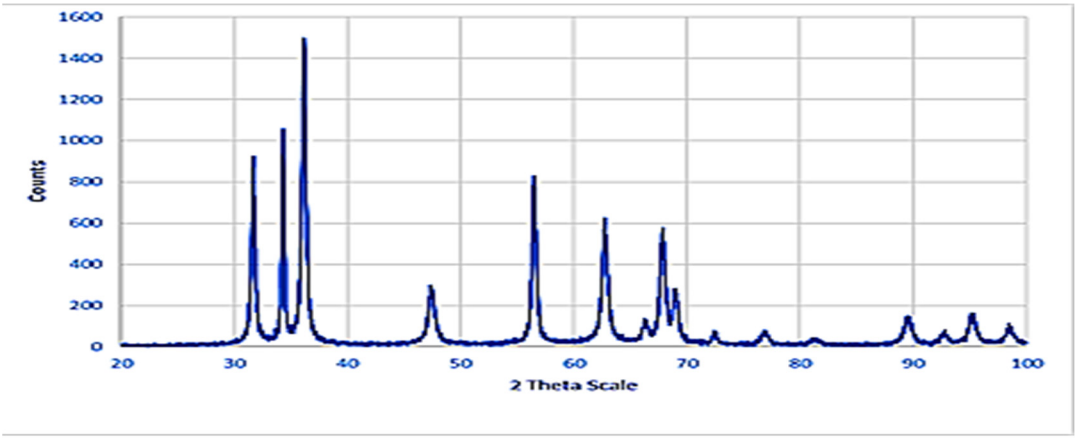

Fig. 4. X-ray diffraction patterns of the green synthesized ZONPs.

XRD Analysis

XRD studies were conducted to determine the crystal phase of the nanoparticles (Figure 4). Intense diffraction peaks were observed at 2θ values of 31.68° , 34.32°, 36.17°, 47.45°, 56.52°, 62.77°, 67.88°, 69.03°, 89.55° and 95.26°, which correspond to the (100), (002), (101), (102), (110), (103), (112), (201), (104), (203) diffraction lattice planes (h, l, k), respectively, confirming the hexagonal structure of the synthesized NPs [23]. These peaks are matched with the code number 96-900-8878 from the XRD software library, and the peaks' pattern is in complete agreement with the reference.

The absence of additional diffraction peaks confirms the phase purity of the ZONPs. Due to the crystalline nature of the synthetic NPs, the available peaks are sharp and the separation between the peaks is excellent, indicating a single-phase crystal structure. The average crystallite size was calculated using Debye–Scherrer's equation, $D = k\lambda / \beta\cos\theta$. In this equation, D represents the average crystallite size, λ is the wavelength of the X-ray (λ=1.54184 Å) for Cu Kα radiation, k is a shape factor typically taken as 0.89, β is the peak full width at half maximum (FWHM) of the diffraction peak, and θ is the Bragg angle. . Using this formula, the average crystalline size of the ZONPs was estimated to be approximately 19.98 nm.

Tyrosinase Inhibitory Activity

The effect of ZONPs on mushroom tyrosinase inhibition was evaluated in different concentrations (62.5–500 µg/ml) (Figure 5). The results showed that the tyrosinase inhibition was increased in a

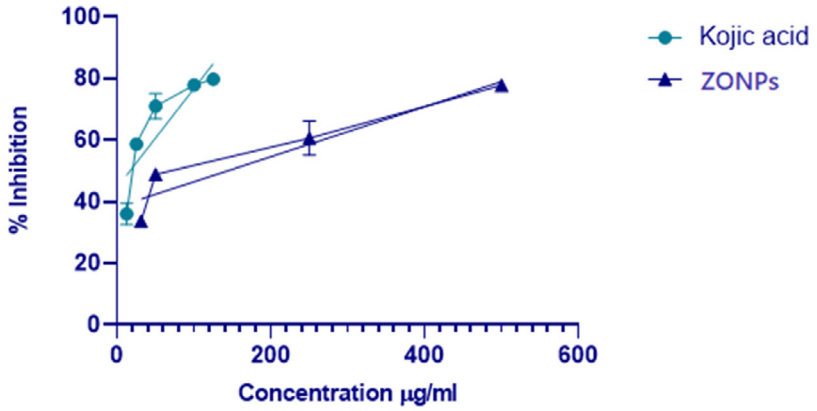

Fig. 5. Tyrosinase inhibitory effects of the green synthesized ZONPs and Kojic acid

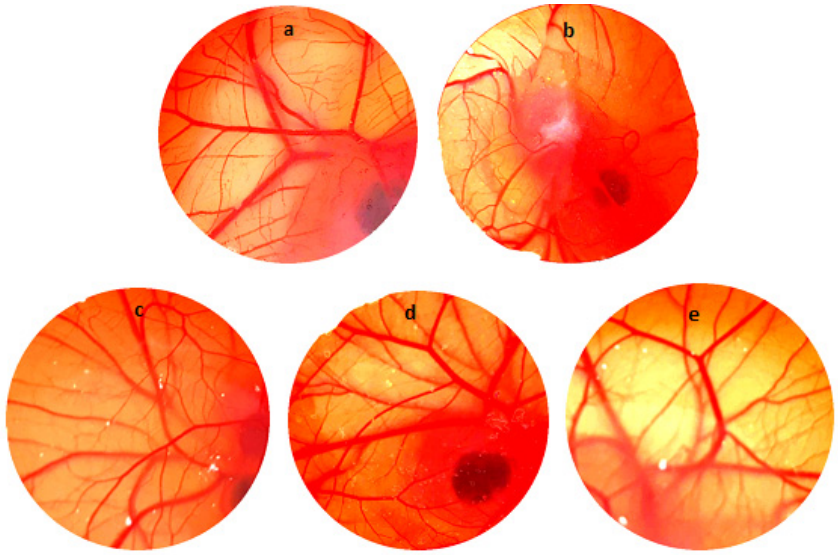

Fig. 6. Representative images showing the angiogenic effects of various treatment groups on CAM assay on day 9. (a) CAM treated with PBS (vehicle control group). (b) CAM treated with 1% DMSO (negative control group). (c) CAM treated with ZONPs at 125 µg/ml. (d) CAM treated with ZONPs at 250 µg/ml. (e) CAM treated with ZONPs at 500 µg/ml.

dose-dependent manner, with an IC_{50} = 143.28 µg/ml. Kojic acid as a positive control showed better anti-tyrosinase activity (IC_{50} = 16.79 µg/ml).

CAM Assay

Angiogenesis activity can be evaluated through CAM assay using angiogenesis indicators, such as the number and length of newly formed arterioles. After treatments on 9-day-old CAMs, each CAM was fixed and photographed (Figure 6). Treatment with ZONPs at 125 and 250 µg/ml increased the number of blood vessels by over 50% compared to the control. In contrast, no significant difference in vessel number was observed between the control group and the group treated with 500 µg/ml ZONPs (Figure 7a). Regarding total vessel length, ZONPs at 125 and 250 µg/ml did not produce a significant change relative to the control, whereas treatment with 500 µg/ml resulted in a 27% reduction (Figure 7b). In the negative control group treated with 1% DMSO, both number and length of vessels showed a significant reduction ($P < 0.001$) (Figures. 8a & b). Based on the CAM assay, the highest concentration of ZONPs significantly suppressed angiogenesis when compared with the group. After the 11-day experimental period, the PBS vehicle control group

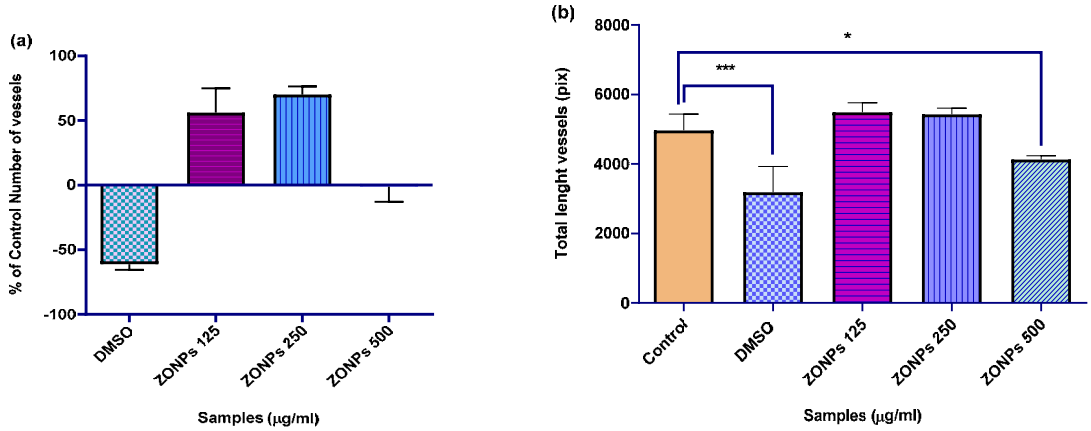

Fig. 7. Results of the morphometric analysis on CAM assay after treatment with the different concentrations of the green synthesized ZONPs and 1% DMSO on day 9 using ImageJ software. (a) % of control number vessels (b) the total length of vessels compared with the control group (PBS). Significant differences compared with the control * ($P < 0.05$); * ** ($P < 0.001$). Data expressed as mean ± SD.

showed no signs of toxicity. In contrast, noticeable morphological alterations were observed in the embryos treated with DMSO and those exposed to 500 µg/mL of ZONPs. The specific data regarding these morphological changes were not presented in the results.

DISCUSSION

Current wound treatments primarily focus on preventing infection and accelerating the hemostasis process; however, patients continue to experience post-treatment complications such as scarring and pigmentation (darkening) at the wound site. Hyperpigmentation often arises during the inflammatory phase and this condition frequently lingers into the proliferation and remodeling stages [17]. During the proliferation phase of wound healing, angiogenesis plays a crucial role as a key biological mechanism that facilitates tissue repair. This process is modulated by multiple growth factors and pro-inflammatory cytokines, which stimulate endothelial cell activation, proliferation, and migration, ultimately leading to the formation of new blood vessels [24]. Nanotechnology, an advanced branch of science that manipulates materials at the nanoscale (1–100 nanometers), provides unique physicochemical properties and innovative applications [15].

In agreement with earlier studies, ZONPs have demonstrated effectiveness in promoting wound healing through multiple mechanisms, including antimicrobial and anti-inflammatory activities, stimulation of cell migration, enhancement of angiogenesis, and facilitation of tissue regeneration [15, 23]. Furthermore, previous findings indicated that ZONPs enhance angiogenesis by downregulating the expression of inflammation-associated genes while upregulating the expression of vascular endothelial growth factor A (VEGF-A) genes [25].

In the present study, ZONPs were synthesized using plant extract along with zinc salt solution. A previous study showed that *P. knappii* is rich in phenolic and flavonoid glycosides [19]. Analysis of the HPLC chromatogram of PAE revealed the contribution of several phytochemicals in the synthesis of ZONPs, which probably had a reducing and stabilizing effect during the green synthesis process. The UV–Vis spectroscopy results confirmed the successful synthesis of ZONPs using PAE, showing a characteristic absorption peak at 373 nm. This observation aligns well with previous studies [26–28]. FTIR analysis revealed the presence of flavonoids and phenolic compounds in the aqueous extract, which played a key role in the reduction, formation, and stabilization of ZONPs [29]. These findings are consistent with earlier published reports [21, 22].

SEM and XRD analyses confirmed that the synthesized ZONPs possessed a well-defined morphology and a pure hexagonal crystalline structure, which is consistent with findings reported in previous studies [26-31]. However, the observed increase in particle size in SEM images was attributed to overlapping and aggregation of nanoparticles. Previous reports have described

that nanoparticle aggregation can reduce the active surface area and alter physicochemical properties, thereby decreasing their penetration into target tissues and cells and ultimately reducing drug delivery efficiency [31, 32]. Additionally, aggregated nanoparticles may provoke immune responses, cause local inflammation, and induce toxicity. To reduce nanoparticle aggregation and improve their biomedical effectiveness, surface modification can be achieved by adjusting factors such as the pH of the solution, reaction temperature and time, and the concentrations of salts and extracts, along with using stabilizing agents like surfactants, water-soluble polymers, or phospholipids [33, 34].

For a long time, tyrosinase inhibitors have been used in cosmetic and medicinal products for the treatment of hyperpigmentation. In this research, the anti-tyrosinase effect of ZONPs was assessed against mushroom tyrosinase, with an IC_{50} of 143.28 µg/ml, which is weaker than that of kojic acid but comparable to the anti-tyrosinase activity previously reported for the use of ZONPs. Ekennia et al. [29] described ZONPs synthesized from *Alchornea laxiflora* leaf extract as having good anti-tyrosinase activity with an IC_{50} of 66.28 µg/ml. In another study, Raajshree et al. [18] found that ZONPs synthesized using *Turbinaria conoides* inhibited tyrosinase activity by nearly 75% at a concentration of 250 µg/ml. The observed differences in tyrosinase inhibitory potency between green-synthesized ZONPs and kojic acid may be attributed to disparities in their physicochemical properties and modes of interaction with the enzyme. Green-synthesized ZONPs are capped with phytochemicals derived from plant extracts, which modify their surface chemistry and impart bioactive functional groups that interact with tyrosinase differently than kojic acid, a small molecule that directly chelates copper ions in the enzyme's active site. Furthermore, the stability and dispersibility of ZONPs influence their inhibitory efficacy, as nanoparticle aggregation reduces the available active surface area [29, 35].

The chicken embryo angiogenesis assay indicated that low concentrations of ZONPs significantly enhanced blood vessel formation without inducing toxicity in treated embryos, suggesting their potential to promote wound healing; however, higher concentrations produced the opposite effect. Previous research has shown that both the angiogenic [36, 37] and anti-angiogenic [38, 39] activities of ZONPs are strongly influenced by their intrinsic characteristics, physicochemical properties, and surrounding environmental conditions [40]. According to Shabestarian et al. [41], the effect of zinc oxide nanoparticles (ZONPs) on angiogenesis is concentration-dependent, as demonstrated by the chorioallantoic membrane (CAM) assay. Within the concentration range of 0 to 500 µg/ml, ZONPs exhibited anti-angiogenic behavior by downregulating the expression of vascular endothelial growth factor (VEGF) and its receptor (VEGFR). Conversely, at concentrations greater than 500 µg/ml, ZONPs indicated pro-angiogenic activity, highlighting the complex role of these nanoparticles in modulating angiogenic processes. However, since high concentrations of ZONPs also induce toxicity in the CAM model, it is critical to carefully optimize the dosage to balance therapeutic angiogenesis modulation with the risk of cytotoxicity. The potential mechanisms behind ZONPs toxicity at higher concentrations in the CAM model likely arise from oxidative stress mediated by reactive oxygen species (ROS), Zn^{2+} ion release, inflammation, and mitochondrial dysfunction leading to cell death. These mechanisms emphasize the importance of dose optimization to ensure the safe therapeutic application of ZONPs [42].

The findings suggest that nanoparticles, depending on the source of reducing agent and concentration, can have a dual role in angiogenesis, thereby emphasizing the need for a more comprehensive investigation of their effects on angiogenic processes to optimize therapeutic outcomes.

CONCLUSIONS

In the present study, green synthesized ZONPs were assessed using *P. knappii* aqueous extract to investigate their anti-tyrosinase and angiogenic effects. The extract served as an effective reducing, capping, and stabilizing agent in the green synthesis of ZONPs. The successful formation of ZONPs was verified through UV–Vis spectroscopy and further supported by FTIR analysis. SEM examination revealed that the nanoparticles exhibited a quasi-spherical morphology and uniform size distribution, while XRD analysis confirmed the crystalline structure, validating the efficiency of the green synthesis method. Evaluation of anti-tyrosinase activity indicated that ZONPs may play a potential role in regulating melanin synthesis by inhibiting tyrosinase; however, additional *in vivo* studies are required

to substantiate the *in vitro* findings. Additionally, the ZONPs can also stimulate angiogenesis, but further investigations are necessary to determine the optimal concentration of ZONPs for maximum effectiveness. Therefore, the ZONPs synthesized from *P. knappii* aqueous extract are recommended as effective pharmaceutical agents in skin whitening cosmetic products and wound healing formulations.

ACKNOWLEDGMENTS

The authors thank the Medicinal Plants Research Center and the Department of Pharmacognosy, Faculty of Pharmacy, Tehran University of Medical Sciences, for their cooperation. This study was supported by the Medicinal Plants Research Center, the Institute of Pharmaceutical Sciences, Faculty of Pharmacy, Tehran University of Medical Sciences, and Tehran, Iran, under the Grant No. 98-01-56-40062.

ETHICAL CONSIDERATIONS

This study was approved by the Ethical Committee of Tehran University of Medical Sciences. ID: IR.TUMS.NIHR.REC.1397.032.

FUNDING

This study was financially supported by a grant from the Medicinal Plants Research Center, the Institute of Pharmaceutical Sciences, Faculty of Pharmacy, Tehran University of Medical Sciences, Tehran, Iran (No. 98-01-56-40062).

CONFLICTS OF INTEREST

The authors declare no conflict of interest.

REFERENCES

1. Dash DK, Panik RK, Sahu AK, Tripathi V. Role of nanobiotechnology in drug discovery development and molecular diagnostic. In Applications of Nanobiotechnology; Stoytcheva M, Zlatev R, Eds.; IntechOpen: London, UK. 2020; pp. 37–43.
2. Joudeh N, Linke D. Nanoparticle classification, physicochemical properties, characterization, and applications: a comprehensive review for biologists. J Nanobiotechnol, 2022; 20(1):262. https://doi.org/10.1186/s12951-022-01477-8
3. Alizadeh N, Salimi A. Multienzymes activity of metals and metal oxide nanomaterials: applications from biotechnology to medicine and environmental engineering. J Nanobiotechnol, 2021; 19(1):26. https://doi.org/10.1186/s12951-021-00771-1
4. Mauricio MD, Guerra-Ojeda S, Marchio P, Valles SL, Aldasoro M, Escribano-Lopez I, Herance JR, Rocha M, et al. Nanoparticles in medicine: a focus on vascular oxidative stress. Oxid Med Cell Longev, 2018; 2018:6231482. https://doi.org/10.1155/2018/6231482
5. Abdelbaky AS, Abd El-Mageed TA, Babalghith AO, Selim S, Mohamed AM. Green synthesis and characterization of ZnO nanoparticles using *Pelargonium odoratissimum* (L.) aqueous leaf extract and their antioxidant, antibacterial and anti-inflammatory activities. Antioxidants, 2022; 11(8):1444. https://doi.org/10.3390/antiox11081444
6. Kumar V, Yadav SK. Plant-mediated synthesis of silver and gold nanoparticles and their applications. J Chem Technol Biotechnol, 2009; 84(2):151–157. https://doi.org/10.1002/jctb.2023
7. Mohanpuria P, Rana NK, Yadav SK. Biosynthesis of nanoparticles: technological concepts and future applications. J Nanoparticle Res, 2008; 10(3):507–517. https://doi.org/10.1007/s11051-007-9141-8
8. Mishra PK, Mishra H, Ekielski A, Talegaonkar S, Vaidya B. Zinc oxide nanoparticles: a promising nanomaterial for biomedical applications. Drug Discov Today, 2017; 22(12):1825-1834. https://doi.org/10.1016/j.drudis.2017.09.011
9. Roy M, Roy A, Rustagi S, Pandey N. An Overview of Nanomaterial Applications in Pharmacology. Biomed Res Int. 2023; 2023:4838043. https://doi.org/10.1155/2023/4838043
10. Wang X, Cao Y. Characterizations of absorption, scattering, and transmission of typical nanoparticles and their suspensions. J Ind Eng Chem, 2020; 82:324–332. https://doi.org/10.1016/j.jiec.2019.10.030
11. Jha S, Rani R & Singh S. Biogenic zinc oxide nanoparticles and their biomedical applications: A review. J Inorg Organomet Polym Mater, 2023; 33:1437–1452. https://doi.org/10.1007/s10904-023-02698-5
12. Vignesh A., Selvakumar S., Vasanth K. Green synthesis and characterization of zinc oxide nanoparticles using Berberis tinctoria Lesch. leaves and fruits extract of multi-biological applications. Nanomed Res J, 2021; 6(2): 128-147. https://doi.org/10.22034/nmrj.2021.02.005
13. Jiménez-Rosado M, Gómez-Zavaglia A, Guerrero Conejo AF, Romero García A. Green synthesis of ZnO nanoparticles using polyphenol extracts from pepper waste (*Capsicum annuum*). J Clean Prod, 2022; 350:131541. https://doi.org/10.1016/j.onano.2022.100067
14. Hassan A, Elebeedy D, Matar ER, Fahmy Mohamed Elsayed A, Abd El Maksoud AI. Investigation of angiogenesis and wound healing potential mechanisms of zinc oxide nanorods. Front Pharmacol, 2021; 12:661217. https://doi.org/10.3389/fphar.2021.661217
15. Asif M, Chaudhry AS, Ashar A, Rashid HB, Saleem MH, Aslam HB, et al. Zinc oxide nanoparticles accelerate the healing of methicillinresistant *Staphylococcus aureus* (MRSA)-infected wounds in rabbits. Asian Pac J Trop Biomed, 2023; 13(11): 488-496. https://doi.org/10.3389/fphar.2021.661217
16. Zhong C, Liang G, Li P, Shi K, Li F, Zhou J, Xu D. Inflammatory response: The target for treating hyperpigmentation during the repair of a burn wound. Front Immunol, 2023; 14:1009137. https://doi.org/10.3389/fimmu.2023.1009137
17. Chadwick S, Heath R, Shah M. Abnormal pigmentation within cutaneous scars: A complication of wound healing. Indian J Plast Surg, 2012;45(2):403-411. https://

doi.org/10.4103/0970-0358.101328
18. Raajshree, Khoushika and Brindha Durairaj. Evaluation of the antityrosinase and antioxidant potential of zinc oxide nanoparticles synthesized from the brown seaweed-*turbinaria conoides*. Int J App Pharm, 2017; 9:116-120. https://doi.org/10.22159/ijap.2017v9i5.20847
19. Sarkhail P, Sarkheil P, Khalighi-Sigaroodi F, Shafiee A, Ostad N. Tyrosinase inhibitor and radical scavenger fractions and isolated compounds from aerial parts of *Peucedanum knappii* Bornm. Nat Prod Res, 2013; 27, 896-9. https://doi.org/10.1080/14786419.2012.665913
20. Janser FA, Ney P, Pinto MT, Langer R, Tschan MP. The chick chorioallantoic membrane (CAM) assay as a three-dimensional model to study autophagy in cancer cells. Bio Protoc, 2019; 9 e3290. https://doi.org/10.21769/BioProtoc.3290
21. Sanaeimehr Z, Javadi I, Namvar F. Antiangiogenic and antiapoptotic effects of green-synthesized zinc oxide nanoparticles using *Sargassum muticum* algae extraction. Cancer Nanotechnol, 2018; 9(1):3. https://doi.org/10.1186/s12645-018-0037-5
22. Barzinjy AA, Azeez HH. Green synthesis and characterization of zinc oxide nanoparticles using *Eucalyptus globulus* Labill. leaf extract and zinc nitrate hexahydrate salt. *SN* Appl Sci, 2020; 2: 991. https://doi.org/10.1007/s42452-020-2813-1
23. Al Mahmood A, Jahan N, Tabassum S, Rahman M, Islam MB, Rahman S, Hossain R. Green synthesis of ZnO and Cu-doped ZnO nanoparticles using Aloe vera gel and investigation of their structural, photocatalytic, and antibacterial properties. Cerâmica, 2024; 70. https://doi.org/eMRCR7435
24. Veith AP, Henderson K, Spencer A, Sligar AD, Baker AB. Therapeutic strategies for enhancing angiogenesis in wound healing. Adv Drug Deliv Rev, 2019; 146: 97-125. https://doi.org/10.1016/j.addr.2018.09.008
25. Alnomasy SF. Antimicrobial, antibiofilm, angiogenesis, anti-inflammatory, and wound healing activities of zinc nanoparticles green synthesized using *Ferula macrecolea* extract. Asian Pac J Trop Biomed, 2024; 14(6): 259-268 https://doi.org/10.4103/apjtb.apjtb_185_24
26. Meena PL, Poswal K, Surela AK. Facile synthesis of ZnO nanoparticles for the effective photodegradation of malachite green dye in aqueous solution. Water Environ J, 2022; 1-12. https://doi.org/10.1111/wej.12783
27. Nawaz HR, Solangi BA, Zehra B, Nadeem U. Preparation of nano zinc oxide and its application in leather as a retanning and antibacterial agent. Canadian J Sci Indus Res, 2011, 2:164-170.
28. Tiwari AK, Jha S, Tripathi SK, et al. Spectroscopic investigations of green synthesized zinc oxide nanoparticles (ZnO NPs): antioxidant and antibacterial activity. Discov Appl Sci. 2024; 6:399. https://doi.org/10.1007/s42452-024-06049-z
29. Ekennia A, Nwaji N, Udeagwu D, Olowu O, Nwanji O, Oje O, Daniel B, Mgbii S, Emma-Uba C. Biosynthesis of zinc oxide nanoparticles using leaf extracts of *Alchornea laxiflora* and its tyrosinase inhibition and catalytic studies. Micron, 2020; 141:102964. https://doi.org/10.1016/j.micron.2020.102964
30. Haghshenas SSP, Nemati A, Simchi R, Kim C-U. Photocatalytic and photoluminescence properties of ZnO/graphene quasi core-shell nanoparticles. Ceram Int, 2019; 45:8945-8961. https://doi.org/10.1016/J.CERAMINT.2019.01.226
31. Perumal P, Sathakkathulla NA, Kumaran K, et al. Green synthesis of zinc oxide nanoparticles using aqueous extract of shilajit and their anticancer activity against HeLa cells. Sci Rep, 2024; 14:2204. https://doi.org/10.1038/s41598-024-2204
32. Ly P-D, Ly K-N, Phan H-L, Nguyen HHT, Duong V-A and Nguyen HV. Recent advances in surface decoration of nanoparticles in drug delivery. Front Nanotechnol, 2024; 6:1456939. https://doi.org/10.3389/fnano.2024.1456939
33. Gherbi B, Laouini SE, Meneceur S, Bouafia A, Hemmami H, Tedjani ML, Thiripuranathar G, Barhoum A, Menaa F. Effect of pH Value on the Bandgap Energy and Particles Size for Biosynthesis of ZnO Nanoparticles: Efficiency for Photocatalytic Adsorption of Methyl Orange. Sustainability, 2022; 14(18):11300. https://doi.org/10.3390/su141811300
34. Ernst LM, Casals E, Italiani P, Boraschi D, Puntes V. The Interactions between Nanoparticles and the Innate Immune System from a Nanotechnologist Perspective. Nanomaterials (Basel). 2021; 11(11):2991. https://doi.org/10.3390/nano11112991
35. Sirelkhatim A, Mahmud S, Seeni A, et al. Review on Zinc Oxide Nanoparticles: Antibacterial activity and toxicity mechanism. Nanomicro Lett. 2015;7(3):219-242. https://doi.org/10.1007/s40820-015-0040-x
36. Barui AK, Veeriah V, Mukherjee S, Manna J, Patel AK, Patra S, Pal K, Murali S, Rana RK, Chatterjee S, et al. Zinc oxide nanoflowers make new blood vessels. Nanoscale, 2012; 4:7861–7869. https://doi.org/10.1039/c2nr32369a
37. Augustine R, Dominic EA, Reju I, Kaimal B, Kalarikkal N, Thomas S. Investigation of angiogenesis and its mechanism using zinc oxide nanoparticle-loaded electrospun tissue engineering scaffolds. RSC Adv, 2014; 4:51528–51536. https://doi.org/10.1039/C4RA09712A
38. Mohammad GRKS, Tabrizi MH, Ardalan T, Yadamani S, Safavi E. Green synthesis of zinc oxide nanoparticles and evaluation of anti-angiogenesis, anti-inflammatory and cytotoxicity properties. J Biosci, 2019; 44:30. PMID: 31180043.
39. Tada-Oikawa S, Ichihara G, Suzuki Y, Izuoka K, Wu W, Yamada Y, et al. Zn (II) released from zinc oxide nano/micro particles suppresses vasculogenesis in human endothelial colony-forming cells. Toxicol Rep, 2015; 2:692-701. https://doi.org/10.1016/j.toxrep.2015.04.003
40. Sukhanova A, Bozrova S, Sokolov P, et al. Dependence of nanoparticle toxicity on their physical and chemical properties. Nanoscale Res Lett, 2018; 13:44. https://doi.org/10.1186/s11671-018-2457-x
41. Shabestarian H, Homayouni Tabrizi M, Movahedi M, Neamati A, Sharifnia F. Green synthesis of Ag-NPs as a metal nanoparticle and ZnO-NPs as a metal oxide nanoparticle: Evaluation of the in vitro cytotoxicity, anti-oxidant, anti-angiogenic activities. Nanomed J, 2023; 10(3): 245-258. https://doi.org/10.22038/nmj.2023.71700.1770
42. Saberi-Hasanabadi P, Malekshah O M, Mohammadi H. The exposure and hazards of zinc oxide nanoparticles: In vitro and in vivo studies. Pharm Biomed Res, 2023; 9 (2):77-84. https://doi.org/10.32598/PBR.9.2.920.2